Elastic-Plastic Analysis of a Propagating Crack under Cyclic Loading

J. C. Newman Jr.*
NASA Langley Research Center, Hampton, Va.

and

Harry Armen Jr.†
Grumman Aerospace Corporation, Bethpage, N.Y.

Fatigue cracks have been experimentally shown to close at positive stresses during constant-amplitude load cycling. The crack-closure phenomenon is caused by residual plastic deformations remaining in the wake of an advancing crack tip. This paper is concerned with the development and application of a two-dimensional finite-element analysis to predict crack-closure and crack-opening stresses during specified histories of cyclic loading. An existing finite-element computer program which accounts for elastic-plastic material behavior under cyclic loading was modified to account for changing boundary conditions—crack growth and intermittent contact of crack surfaces. This program was subsequently used to study the crack-closure behavior under constant-amplitude and simple block-program loading.

Nomenclature

a = half length of crack, meters
$[B]$ = matrix relating total strains to nodal displacements, meters^{-1}
$\{F\}$ = generalized load vector ($=\{P\}+\{Q\}+\{R\}$), Newtons
f = von Mises yield condition
$[K]$ = elastic stiffness matrix, N/m
$\{P\}$ = applied load vector, Newtons
$\{Q\}$ = "effective" plastic load vector, Newtons
$\{R\}$ = equilibrium imbalance vector, Newtons
S = applied gross stress, N/m^2
S_O = crack-opening stress, N/m^2
S_{Oj} = stabilized crack-opening stress for stress level S_{max}, N/m^2
S_{maxj} = maximum applied stress for level j, N/m^2
S_{minj} = minimum applied stress for level j, N/m^2
$\{u\}$ = generalized nodal displacements, meters
u,v = displacements in x and y direction, respectively, meters
W = plate width, meters
x,y = coordinate system
Δa = crack-growth increment, meters
ΔN = incremental number of cycles
$\{\Delta P\}$ = applied load increment, Newtons
$\{\Delta\epsilon\}$ = total strain increment
$\Delta\epsilon_{all}$ = maximum allowable strain increment
$\{\Delta\epsilon_p\}$ = plastic strain increment
$\{\Delta\sigma\}$ = stress increment, N/m^2
$\{\epsilon\}$ = total strain components
$\{\epsilon_e\}$ = elastic strain components
$\{\epsilon_p\}$ = plastic strain components
$\{\sigma\}$ = stress components, N/m^2
σ_{yy} = normal stress in y-direction, N/m^2

Presented as Paper 74-366 at the AIAA/ASME/SAE 15th Structures, Structural Dynamics and Materials Conference, Las Vegas, Nevada, April 17-19, 1974; submitted July 2, 1974; revision received December 24, 1974. The authors wish to thank A. Pifko and H. Levine, Grumman Aerospace corporation, for their aid associated with the finite-element aspects of this program, and the staff of the Analytical Computing Division, NASA Langley Research Center, for their aid in implementing and improving the efficiency of the program. The authors also acknowledge the valuable discussions with W. Elber, NASA Langley Research Center, and A. Wolfman, Grumman Aerospace Corporation, concerning the phenomena associated with fatigue-crack closure.

Index categories: Aircraft Structural Design (including Loads); Structural Static Analysis.

*Research Engineer, Structural Integrity Branch.

†Head, Applied Mechanics Group, Research Department. Member AIAA.

Introduction

FATIGUE-crack propagation was, until recently, assumed to be directly related to the linear elastic-stress-intensity factor range during cyclic loading. Implicit in this concept were the assumptions that only the tensile portion of the load cycle was effective in growing the crack and that cracks close only at zero load. Elber[1,2] has shown experimentally that fatigue cracks close at positive loads during constant-amplitude load cycling. He has indicated that fatigue-crack closure may be a significant factor in causing the stress-interaction effects on crack-growth rates (retardation or acceleration) under general cyclic loading. He has also postulated that the crack-closure phenomenon, associated with a growing crack under cyclic loading, was caused by residual plastic deformations remaining in the wake of the advancing crack tip.

The analytical model for an extending crack under cyclic loading must be able to account for the changing kinematic boundary conditions associated with crack growth and the intermittent contact and separation of the crack surfaces during a specified load history. These changing boundary conditions must also be incorporated into the equations that govern the nonlinear load-deformation behavior of the structure. These requirements—an extending crack and nonlinear material behavior—are well suited for the finite-element method.

The steadily growing crack under monotonically increasing load has previously been treated in Refs. 3 and 4 using the finite-element method. However, these investigations did not allow for cyclic loads to be applied and, consequently, the occurrence of crack closure.

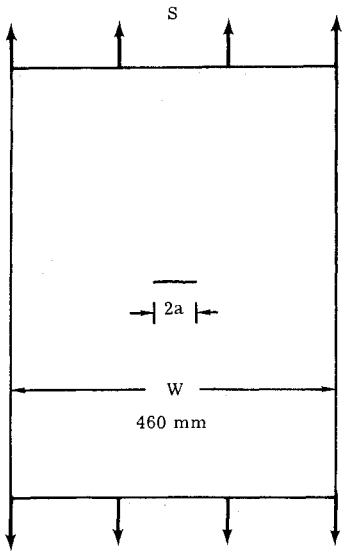

Fig. 1 Center-crack panel subjected to uniform stress.

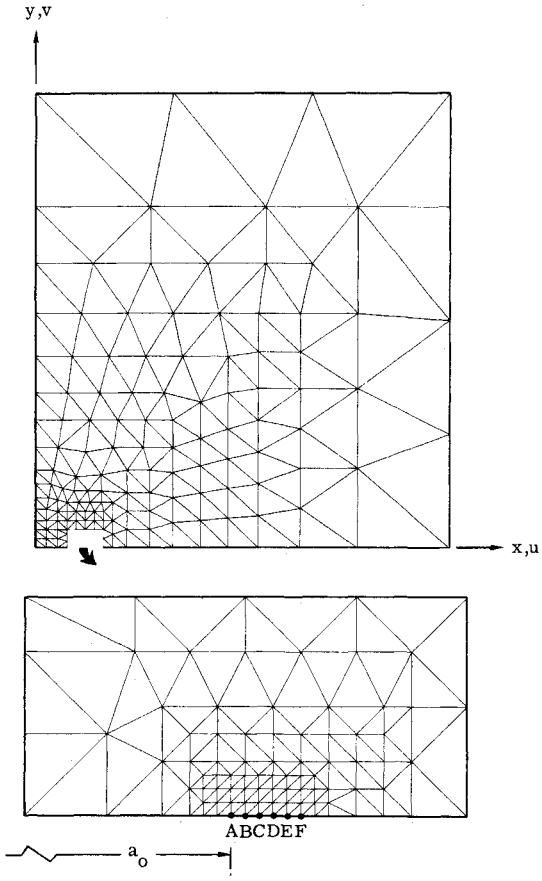

Fig. 2 Finite-element idealization of the center-crack panel.

The present paper is concerned with the development and application of a two-dimensional, nonlinear, finite-element program (generalized plane stress) to study fatigue-crack growth under cyclic loading. An existing finite-element program[5,6] which accounts for nonlinear material behavior under cyclic loading was modified to account for changing boundary conditions—crack growth and intermittent contact of crack surfaces. The modified finite-element program incorporated a procedure for the efficient reanalysis of structures which undergo changes in kinematic boundary conditions or material properties. The reanalysis procedure, originally presented in Refs. 7 and 8, is a substructuring technique that allows efficient modification of the structural stiffness matrix. This procedure has the advantage that the original stiffness matrix does not have to be reformulated whenever a crack extends, closes, or separates.

The finite-element program which includes the capability of accounting for crack growth under cyclic loading was used to study the crack-growth and crack-closure behavior in a center-cracked panel, Fig. 1. The finite-element model of the center-crack panel is shown in Fig. 2. The finite-element model was assumed to be an elastic-perfectly plastic material and was subjected to either constant-amplitude or simple block-program loading. (The finite-element program can also handle either linear or nonlinear strain-hardening materials.) In the analysis, no attempt was made to establish a failure criterion for crack growth. Crack growth was simulated by releasing one node during each cycle at the maximum applied stress. Therefore, the results obtained herein should only be considered as trends in crack-growth behavior and represents an initial attempt to analytically determine crack-closure and crack-opening stresses. For constant-amplitude loading, the model was subjected to various stress levels and stress ratios (ratio of minimum to maximum stress). For simple block-program loading, the panel was subjected to two sequences of two-level block-program loading. These sequences were either high-to-low or low-to-high block-program loading. The crack-closure stresses, crack-opening stresses, displacements, and residual stress distributions in the crack-tip region were determined as a function of applied stress.

Finite-Element Analysis

The approach selected here for the elastic-plastic analysis of a cracked plate, Fig. 1, employed the finite-element method using the initial-strain concept as described in Refs. 5 and 6. In this approach, the load-displacement relations are written to include the effects of initial strains. The plastic strains are interpreted as initial strains and, together with the constitutive relations for an elastic-plastic material, produce an effective plastic-load vector. The plastic-load vectors are applied to any element which has become plastic and maintain the plastic deformations on that particular elements while the external loads are applied. For each element the plastic-load vectors are self-equilibrating. The finite-element model was composed of constant-strain triangular elements. The governing matrix equations and the nonlinear constitutive relations are given in Refs. 5 and 6. The governing equations are only briefly reviewed here in the context of the modifications required to treat crack growth and intermittent contact or separation of crack surfaces.

In general, the matrix equation that governs the response of a discretized structure under loads which cause plastic deformation can be written as

$$[K]\ \{u\} = \{P\} + \{Q\} + \{R\} = \{F\} \tag{1}$$

where $[K]$ is the conventional elastic stiffness matrix, $\{u\}$ is the generalized nodal displacements, $\{P\}$ is the applied load vector, $\{Q\}$ is the "effective" plastic load vector, and $\{R\}$ is an equilibrium imbalance vector that may exist as a result of the incremental linearization of the nonlinear equations.[9]

For small deformations, the total strain components in any element were decomposed into elastic and plastic strain components as

$$\{\epsilon\} = \{\epsilon_e\} + \{\epsilon_p\} \tag{2}$$

The plastic strain components were used to compute the plastic load vector as

$$\{Q\} = \sum_{n=1}^{N} [\bar{K}]\ \{\epsilon_p\} \tag{3}$$

where $[\bar{K}]$ is the initial-strain matrix for an individual element. The summation extends over those elements that are in a plastic state.[5,6]

Solution Procedure for the Unmodified Structure

For elasto-plastic analyses, it is generally necessary to apply loads incrementally to satisfy the appropriate yield condition (von Mises) and flow rule associated with incremental plasticity.[5] The procedure used for a typical load increment is summarized as follows: 1) Apply load increment $\{\Delta P\}$ and determine the nodal displacements $\{u\}$ from Eq. (1); initially $\{Q\}=\{R\}=0$; 2) Compute total strains $\{\epsilon\}$ and increments of total strain $\{\Delta\epsilon\}$ from the appropriate strain-displacement relation ($\{\epsilon\}=[B]\ \{u\}$); 3) Compute increments of stress $\{\Delta\sigma\}$ and add to current stress $\{\sigma\}$. Check yield condition for plastic elements; 4) Compute increments of plastic strain $\{\Delta\epsilon_p\}$ from the total strain increments $\{\Delta\epsilon\}$ for elements in plastic state; 5) Compute the plastic load vector $\{Q\}$ and the equilibrium imbalance vector $\{R\}$ for elements which are in the plastic state; 6) Add load increment $\{\Delta P\}$ to applied load vector $\{P\}$ and repeat steps 1-5 until the desired load is reached. Input new load.

From an incremental analysis, the plastic strains and, hence, the plastic load vector at load increment i could not be determined without a prior knowledge of the displacements after load increment i. Thus, the plastic load vector was computed from the displacements in the preceding increment and, consequently, was underestimated. Therefore, the equilibrium imbalance vector $\{R\}$ was added to the applied and plastic load vectors to approximately correct for the errors associated with the incremental linearization of the nonlinear equations (that is, computing $\{Q\}$ from displacements obtained in the preceding increment). The errors associated with incremental linearization are reduced by using a sufficiently small load increment. In this paper, the linearization errors were approximately accounted for, first, by using relatively small load increments (ΔP was 5% of the load required to yield first element) and, second, by setting

$$\{R\}=\sum_{n=1}^{N}[\bar{K}]\ \{\Delta\epsilon_p\}^{i-1} \tag{4}$$

where $\{\Delta\epsilon_p\}$ are the increments of plastic strain computed from the preceding increment. Thus, the final form of Eq. (1) was

$$[K]\ \{u\}^i=\{P\}^i+\{Q\}^{i-1}+\{R\} \tag{5}$$

where i and $i-1$ are the current and preceding load increments, respectively.

After each load increment, a loading criterion was monitored to determine whether an element was loading or unloading. For ideally plastic behavior, if we express the yield condition as a function of stress $f(\sigma)$, then the condition for loading and unloading was given by

$$\left\{\frac{\partial f}{\partial\{\sigma\}}\right\}^T\{\Delta\sigma\}\ \begin{matrix}=0 \text{ loading}\\ <0 \text{ unloading}\end{matrix} \tag{6}$$

The superscript T denotes the matrix transpose. Elements which are unloading are treated elastically.

Solution Procedure for the Modified Structure

As previously mentioned, the finite-element analysis of a growing crack under cyclic loading must be able to account for changing boundary conditions during a specified load history. A procedure[7,8] for modifying a structure by adding or deleting certain degrees of freedom (changing boundary conditions) was incorporated into the nonlinear analysis program. This procedure is briefly described as follows.

Equation (1) was partitioned into the form

$$\left[\begin{array}{c|c}K_{aa} & K_{ab}\\ \hline K_{ba} & K_{bb}\end{array}\right]\left\{\begin{array}{c}u_a\\ \hline u_b\end{array}\right\}=\left\{\begin{array}{c}P_a\\ \hline P_b\end{array}\right\}$$

$$+\left\{\begin{array}{c}Q_a\\ \hline Q_b\end{array}\right\}+\left\{\begin{array}{c}R_a\\ \hline R_b\end{array}\right\}=\left\{\begin{array}{c}F_a\\ \hline F_b\end{array}\right\} \tag{7}$$

where the subscript "a" refers to the unmodified degrees of freedom and "b" denotes those which are to be modified. The modified degrees of freedom are either those which were originally restrained against motion but are now allowed to displace (crack growth or crack opening) or those which were originally allowed to displace but are now restrained from motion (crack closure). Equation (7) was expanded into

$$[K_{aa}]\ \{u_a\}+[K_{ab}]\ \{u_b\}=\{F_a\}$$

$$[K_{ba}]\ \{u_a\}+[K_{bb}]\ \{u_b\}=\{F_b\} \tag{8}$$

The solution to Eqs. (8) provided the displacements for the modified structure. The details associated with determining the modified displacements are described in the Appendix. The procedure for modifying part of the stiffness matrix, $[K_{ab}]$ and $[K_{bb}]$, has the advantage that the unmodified stiffness matrix $[K_{aa}]$ which is generally much larger than the matrix $[K_{bb}]$, does not have to be reformulated and decomposed whenever the crack grows, closes, or separates. Thus, a solution technique such as the Cholesky decomposition[10] of a symmetric, positive-definite matrix needs to be performed only once on the stiffness matrix $[K_{aa}]$. The incorporation of this technique into the existing nonlinear finite-element program for the analysis of membrance stressed structures provided an efficient tool to analyze cyclic crack growth. Efficiency was claimed on the basis of reducing the number of computer operations required to release or close a node (or nodes). The number of operations required to modify the stiffness matrix was given by[7]

$$M+n(Bn_r/2+n_r^2/4)+(n_r^3/6) \tag{9}$$

where M is the operation count, n is the total number of degrees of freedom of the modified structure, n_r is the degrees of freedom to be modified, and B is the semibandwidth of the stiffness matrix. The break-even point for this procedure vs a complete reformulation occurs when $n_r=0.75\,B$. For the stiffness matrix considered in this paper n_r was approximately $0.1\,B$. Thus, a considerable savings in computer time was obtained each time a node was released or closed when compared with the operations required for a complete reformulation of the stiffness matrix.

The procedure for treating both nonlinear material behavior and changing boundary conditions remains unchanged from that previously presented for the unmodified structure, except that the flow of operation was interrupted between steps 1 and 2. All nodal displacements along the crack line were monitored to determine whether the nodes were to be released (crack growth), remain open (crack opening), or remain closed (crack closure). The modified displacements associated with these decisions were then computed.

To extend the crack, the crack-tip node was arbitrarily chosen to be released at maximum load and the crack tip advanced to the next node. No attempt was made to establish a failure criterion for crack growth. During this process, the nodal force carried by the crack-tip node was suddenly released. Equation (6) was monitored to determine which elements were unloading and which were loading. To insure that the stresses and total strain increments in the adjacent elements satisfy the appropriate yield condition and flow rule, two additional computational procedures were incorporated to account for the sudden jump in response of the structure.

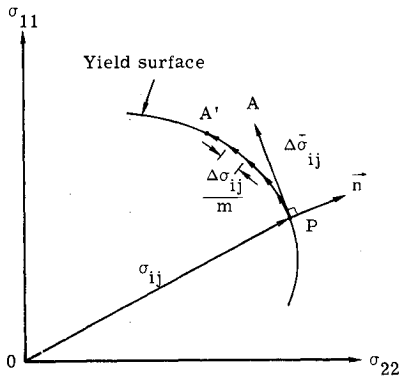

Fig. 3 Yield surface in two-dimensional stress space.

These procedures are 1) a subincrementation technique to account for large total strain increments developed near the crack tip, and 2) an iterative scheme to redistribute the force previously carried by the broken node. A discussion of these procedures follows.

The flow theories of plasticity generally lead to constitutive equations relating increments of stress to increments of plastic strain. Implicit in these relations is the restriction that plastic deformation must proceed in small increments of stress and strain. This restriction is illustrated in Fig. 3 for the $\sigma_{11}-\sigma_{22}$ stress space of an elastic-perfectly plastic material. Assuming that point p represents the state of stress σ_{ij} on the yield surface, then the flow rule for an elastic-perfectly plastic material states that the stress increment $\Delta\sigma_{ij}$ must be directed along the tangent to the yield surface. However, large values of $\Delta\sigma_{ij}$ (caused by large increments in total strain) such as that shown in Fig. 3 as $\Delta\bar{\sigma}_{ij}$ results in a final stress state (point A) that is not acceptable. The subincrementation procedure used here was based on that presented in Ref. 11, where the largest increment in total strain on any element was divided by a maximum allowable value, $\Delta\epsilon_{all}$, to give

$$m=(\Delta\epsilon_{max}/\Delta\epsilon_{all}) \tag{10}$$

where $\Delta\epsilon_{max}$ was the largest of the three strain components. If $\Delta\epsilon_{max}$ was less than $\Delta\epsilon_{all}$, m was set to unity. The value of m represents the number of subincrements used during the process to release a node. The values of $\Delta\epsilon_{all}$ used here was based on the following relation

$$\Delta\epsilon_{all}=\epsilon_o(\Delta P/P_{ys}) \tag{11}$$

where ϵ_0 is the tensile yield strain of the material, ΔP is the load increment, and P_{ys} is the load at which initial yielding begins at some point in the structure. The subincrementation procedure maintains an acceptable stress state (i.e., on the yield surface) such as A' in Fig. 3.

The second inaccuracy associated with crack extension was in determining the stabilized plastic load vector in Eq. (5). Assuming that the i^{th} increment represents the point at which the crack grows, then the plastic load vectors computed from the displacements in the preceding increment are not an accurate representation of the plastic state after the crack grows. Consequently, an iterative procedure was introduced to determine the corresponding states of plastic strain and displacement. This procedure is illustrated for load increment i in the following equation

$$[K]\ \{u\}_I^i=\{P\}^i+\{Q\}_{I-1}^{i-1} \tag{12}$$

where the subscript represents the I^{th} iteration. The iterative process was repeated until there was less than 1% change in the displacements between any two iterative steps. The iterative process required between 5 and 15 iterations to stabilize the plastic load vector. During the iterative process the applied vector $\{P\}^i$ was held constant at maximum load and the equilibrium imbalance vector $\{R\}$ was set to zero.

Application of the Finite-Element Analysis to Cyclic Crack Growth

Elber,[2] on the basis of fatigue crack-closure experiments under constant-amplitude loading on 2024-T3 aluminum alloy materials, proposed the following equation for fatigue crack propagation rates

$$(\Delta a/\Delta N)=c\ \Delta K_{eff}^n \tag{13}$$

where c,n are material constants and ΔK_{eff} was the effective stress-intensity factor range. He proposed that the effective stress-intensity range be calculated by

$$\Delta K_{eff}=(S_{max}-S_O)\ (\pi a)^{1/2}\alpha \tag{14}$$

where S_{max} was the maximum stress, S_O was the crack-opening stress, and α was a boundary-correction factor. Thus, the crack was assumed to propagate only during that portion of the load cycle for which it was fully open. Therefore under both constant- and variable-amplitude loading, the crack-closure and crack-opening stresses may be significant factors in the crack-growth mechanism.

The modified finite-element program was used to study the crack-growth and crack-closure behavior in a model of the center-cracked panel. The finite-element idealization and the coordinate system used for the center-cracked panel are shown in Fig. 2. The initial crack half length a_o was 27.3 mm and the total panel width was 460 mm. The initial crack tip was located at node A (see Fig. 2). The elastic-stress concentration (ratio of σ_{yy} in the highest stressed crack-tip element to the applied stress) for this idealization was 7.2. The panel material was assumed to be elastic-perfectly plastic, with a tensile (and compressive) yield stress equal to 550 MN/m^2 and a modulus of elasticity of 72,300 MN/m^2. These properties simulated a high-strength aluminum alloy material.

The following sections give the results of applying the finite-element program to an extending crack under cyclic loading. The center-cracked panel was subjected to either constant-amplitude or simple block-program loading. In this paper, no attempt has been made to establish a failure criterion for crack growth. For any cyclic loading, the crack-tip node (A, B..., F in Fig. 2) was arbitrarily chosen to be released at maximum applied stress regardless of the magnitude of the applied stress and of any prior stress history. Thus, the model provides no direct information on the amount of crack growth per cycle; this information must be obtained from Eq. (13). Instead, the analysis provides only the crack-opening stress S_O to be used in Eq. (14). Of course, the accuracy of the calculated crack-opening stress would be affected by the finite-element grid size chosen to model the crack tip. A finer element mesh, than that used here, would give more accurate results for S_O and would also give crack-growth increments per cycle in closer agreement with experimental results. Therefore, the results on crack-closure and crack-opening stresses, presented here, should only be considered as trends and represents an initial attempt to analytically determine crack-closure effects. Further studies are planned to investigate the crack-closure effects using element-mesh sizes an order of magnitude smaller than that used here.

Crack Growth Under Constant-Amplitude Loading

Stress Level

The constant-amplitude loading applied to the center-crack panel is shown in Fig. 4. The maximum stress was 170 MN/m^2. As the cyclic stresses were applied, the crack initially opened at an infinitesimal stress, and x indicates the point at which the highest stressed crack-tip element initially yields. At maximum stress, node A was allowed to displace (crack growth) and the crack tip advanced to node B. During

unloading, node A was found to close at a positive stress (solid symbol) and was constrained against further motion. When the panel was reloaded, node A opened (open symbol) at approximately the same stress at which it had previously closed. Again, upon reaching the maximum stress, another node B was allowed to displace. During unloading, node B closed at a slightly higher stress than had occurred at node A on the previous cycle. Further cycling indicated approximately the same closure and opening stresses. The crack-opening stresses were approximately 30% of the maximum applied stress.

To investigate the influence of a higher stress level, than previously presented, on the crack-closure phenomenon, Fig. 5 shows the results of constant-amplitude crack growth with $S_{max1} = 260$ MN/m^2. Again, the solid and open symbols indicate crack closure and opening stresses, respectively. However, in this case, the contact (closure) stresses near node A (after the first cycle) were so large that the material behind the crack tip yielded in compression and the subsequent opening stress was considerably lower than the previous closure stress. The closure stress remained nearly constant during further cycling but the opening stress increased after each cycle. The opening stress converged to the previously established closure stress which was approximately 45% of the maximum applied stress. The magnitude of the maximum applied stress seems to establish the crack-closure stress. Then, with sufficient number of cycles, the opening stress seems to converge to the previously established closure stress.

The crack surface displacements for the constant-amplitude crack growth shown in Fig. 5 for $S_{max1} = 260$ MN/m^2 are shown in Fig. 6. The displacements, v, in the y direction are plotted against the coordinate location. The lower curve shows the displacements at maximum stress with the crack tip located at node A (no crack growth had occurred). The other curves indicate the crack-opening displacements at the maximum applied stress after each increment of crack growth. The sharp knee (slightly behind node A) in the displacement curves indicates the beginning of severe plastic deformation.

Figure 7 shows the crack-opening displacements as the panel was unloaded from the maximum applied stress with the crack tip at node E. The solid curve shows the displacements at the maximum stress after 4 increments of crack extension. The dash-dot curve shows the displacements at maximum stress for which no cyclic crack growth has occurred (crack tip node E). The shaded region shows the permanent plastic deformation left behind as the crack tip advanced. It was this plastic deformation which caused the crack surfaces to close before the panel was fully unloaded. At a stress of 120 MN/m^2, the crack surface at node D closes and was constrained against further motion. After further unloading, the displacements at zero stress show that all previous crack-tip nodes have closed and the crack surface behind node A has remained open. The local crack-tip stresses at maximum load and the residual stresses during unloading are shown in Fig. 8.

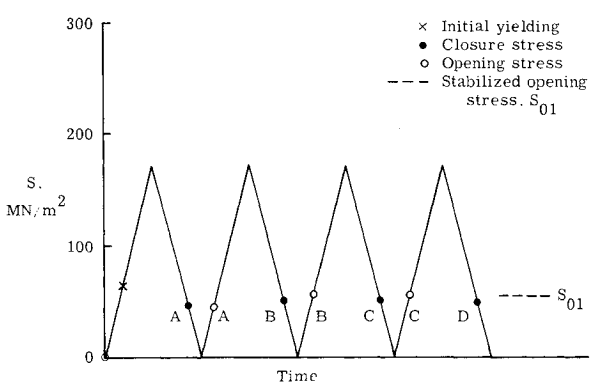

Fig. 4 Constant-amplitude crack growth with $S_{max1} = 170$ MN/m^2.

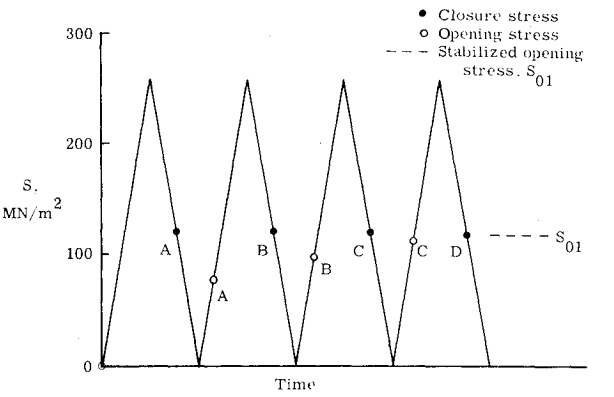

Fig. 5 Constant-amplitude crack growth with $S_{max1} = 260$ MN/m^2.

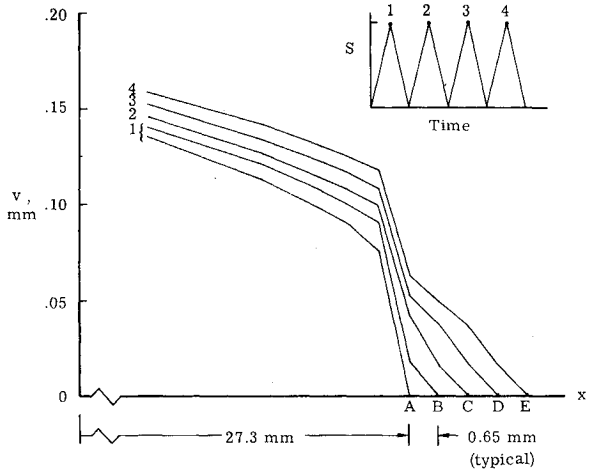

Fig. 6 Crack surface displacements under constant-amplitude crack growth with $S_{max1} = 260$ MN/m^2.

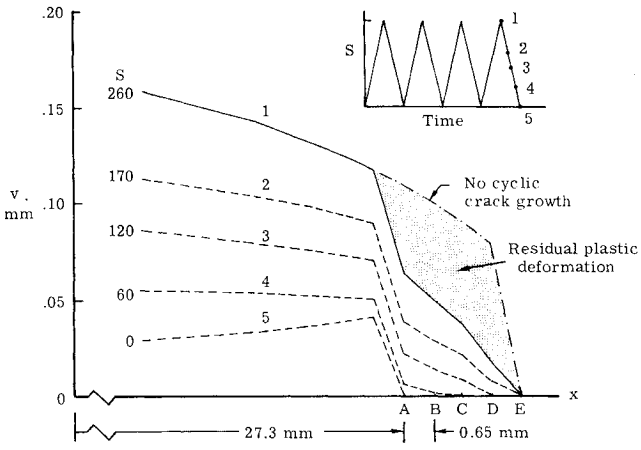

Fig. 7 Crack surface displacements during unloading after constant-amplitude crack growth ($S_{max1} = 260$ MN/m^2).

At maximum load, the crack-tip stresses reach a plateau in front of the crack tip (characteristic of an elastic-perfectly plastic material). Because the stresses are computed at the centroid of the elements (≈ 0.3 mm from the crack surface), the stresses do not immediately drop to zero behind the crack tip. During further unloading, the contact stresses along the crack surfaces (near the crack tip) were large enough to cause the material to yield in compression.

Stress Ratio

The previous cyclic stress history had a stress ratio (minimum stress to maximum stress) of zero. The next cyclic

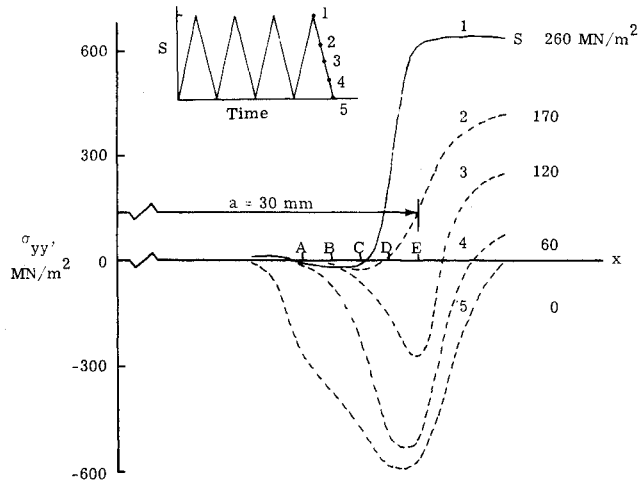

Fig. 8 Local crack tip stress distributions during unloading after constant-amplitude crack growth ($S_{max1} = 260$ MN/m^2).

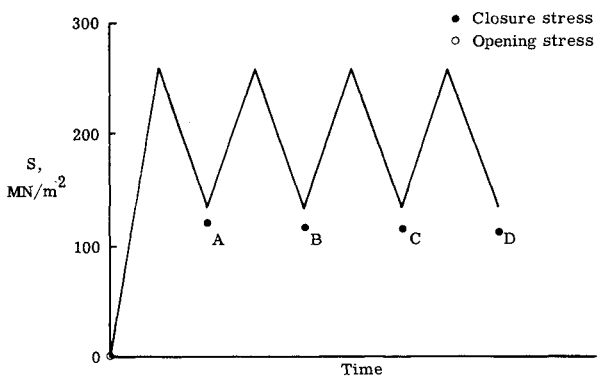

Fig. 9 Constant-amplitude crack growth with $S_{max1} = 260$ MN/m^2 and $S_{min1} = 130$ MN/m^2.

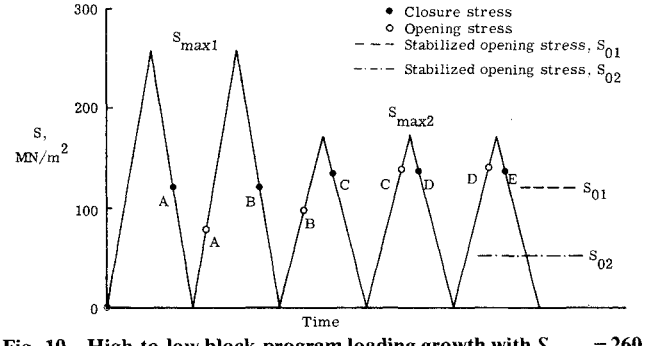

Fig. 10 High-to-low block-program loading growth with $S_{max1} = 260$ MN/m^2 and $S_{max2} = 170$ MN/m^2.

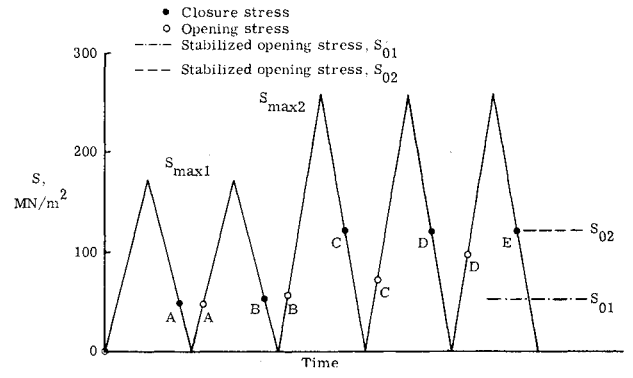

Fig. 11 Low-to-high block-program loading crack growth with $S_{max1} = 170$ MN/m^2 and $S_{max2} = 260$ MN/m^2.

stress history (Fig. 9) had a maximum stress of 260 MN/m^2 and a minimum stress of 130 MN/m^2 (or a stress ratio of 0.5). Again, nodes *A*, *B*, *C*, and *D* were released at maximum stress. But in this case, the crack surfaces never closed. The solid symbols denote what the closure stress would have been if the panel had been allowed to unload beyond the minimum stress. If crack propagation rates are related to the effective stress-intensity [Eq. (12)], then the crack-growth rates should be independent of the closure or opening stresses for stress ratios greater than 0.45 for $S_{max1} = 260$ MN/m^2. These results are consistent with the experimental results obtained by Katcher[12] in which the crack-opening stresses were found to be lower than the minimum stress for stress ratios greater than approximately 0.3 for 2219-T851 aluminum alloy material.

Crack Growth Under Simple Block-Program Loading

High-to-Low Block Loading

The high-to-low block-program loading applied to the center-crack panel is shown in Fig. 10. The maximum stress S_{max1} (first block) was 260 MN/m^2 and S_{max2} (second block) was 170 MN/m^2. The crack-closure and crack-opening stresses for the two cycles of S_{max1} were identical to those previously shown in Fig. 5. Note that the opening and closure stresses for S_{max1} had not yet stabilized. At the maximum stress S_{max2}, node *C* was allowed to displace. During unloading, node *C* closed at a stress which was approximately 10% higher than the stabilized opening stress (S_{01}) for S_{max1} (dashed line). When the panel was reloaded, node *C* opened at a stress slightly higher than the stress at which it had previously closed. During further cycling, nodes opened and closed at about the same stresses that were previously observed. If more than 3 cycles of S_{max2} had been applied, the closure and opening stresses would be expected to decrease as the crack grows and would be expected to converge to the dash-dot line (S_{02}, the stabilized opening stress for S_{max2}) as the crack grows out of the material yielded by S_{max1}. Because the opening stresses for S_{max2} are considerably higher than S_{02}, the crack-growth rates [computed from Eq. (12)] would be considerably slower than if the 2 cycles of S_{max1} had not been applied. This behavior has been experimentally observed and is referred to as crack-growth retardation.

Low-to-High Block Loading

The low-to-high block-program loading applied to the center-crack panel is shown in Fig. 11. In contrast to the previous cyclic history, the first 2 cycles of S_{max1} were at 170 MN/m^2 and the three cycles of S_{max2} were at 260 MN/m^2. Again, the crack closure and opening stress for the 2 cycles of S_{max1} were identical to that shown in Fig. 4. At the first maximum stress S_{max2}, node *C* was released. When the plate was unloaded, node *C* closed at a stress which was approximately 45% of the maximum stress. At zero stress, the material near node *C* yielded in compression and the subsequent opening stress was lower than the previous closure stress. Further cycling showed that the closure stress remained nearly constant while the opening stress increased after each cycle. Although only three cycles of S_{max2} were applied, the opening stresses are expected to converge to the stabilized opening stress (S_{02}) for S_{max2} (dashed line) similar to that observed in Fig. 5. Because the opening stresses for S_{max2} are lower than the stabilized opening stress S_{02}, the crack-growth rates [computed from Eq. (12)] would be faster than the crack-growth rates computed using the stabilized opening stress S_{02}. This behavior in crack-growth rates has also been experimentally observed and is referred to as crack-growth acceleration.[13]

Conclusions

A two-dimensional (plane stress) finite-element program which accounts for nonlinear material behavior under cyclic loading has been modified to account for changing boundary conditions—crack growth and intermittent contact of crack

surfaces. The finite-element program also incorporated an efficient procedure for the reanalysis of structures which undergo changes in boundary conditions. This program was used to study the cyclic crack-growth and closure behavior in a center-crack panel. The finite-element model of the panel was assumed to be an elastic-perfectly plastic material and was subjected to either constant-amplitude or simple block-program loading.

Although the failure criterion used in growing the crack was arbitrary and the crack-growth increments per cycle were very large compared to experimental results, the calculated crack-opening stresses under either constant-amplitude or simple block-program loading were qualitatively consistent with experimental observations. That is, fatigue cracks open at approximately 0.3-0.5 of the maximum applied stress. The crack-opening stresses, when used with Elber's crack-growth equation, also gave crack-growth rates which were qualitatively consistent with experimental observations (retardation or acceleration). Thus, the finite-element analysis of crack growth which includes the effects of crack closure and crack opening should give further insight into the fatigue-crack-growth mechanism. Further studies with finer grid sizes, than that used here, are needed in order to more accurately determine how crack-opening stresses vary as a function of stress level, stress ratio (S_{min}/S_{max}) and stress history.

Appendix: Determination of Displacements for the Modified Structure

This section describes the procedure to modify a structure by the addition or deletion of certain degrees of freedom. Of course, the modified displacements could be found by a complete reanalysis (including reassembly) using the modified stiffness influence coefficients. However, for localized changes, such as crack growth or crack closure, complete reanalysis would be very uneconomical.

Recalling that Eq. (1) was partitioned into the form

$$\begin{bmatrix} K_{aa} & K_{ab} \\ K_{ba} & K_{bb} \end{bmatrix} \begin{Bmatrix} u_a \\ u_b \end{Bmatrix} = \begin{Bmatrix} F_a \\ F_b \end{Bmatrix} \tag{A1}$$

where the subscript "a" refers to the unmodified degrees of freedom and "b" to those that are to be modified (i.e., nodes originally restrained against motion but are not allowed to displace). Equation (A1) was expanded into

$$[K_{aa}]\ \{u_a\} + [K_{ab}]\ \{u_b\} = \{F_a\} \tag{A2}$$

$$[K_{ba}]\ \{u_a\} + [K_{bb}]\ \{u_b\} = \{F_b\} \tag{A3}$$

Initially the displacements $\{u_b\}$ are assumed to be zero and the solution to Eq. (A2) gives the displacement $\{\bar{u}_a\}$ for the unmodified structure as

$$\{\bar{u}_a\} = [K_{aa}]^{-1}\ \{F_a\} \tag{A4}$$

By means of the Cholesky decompositon[10] of a symmetric, positive-definite matrix, the stiffness matric $[K_{aa}]$ was written as

$$[K_{aa}] = [L]\ [L]^T \tag{A5}$$

where $[L]$ is a lower triangular array, and the superscript T indicates the matrix transpose. Thus, the inverse of $[K_{aa}]$ was

$$[K_{aa}]^{-1} = [L]^{-T}\ [L]^{-1} \tag{A6}$$

The Cholesky decomposition of matrix $[K_{aa}]$ was performed only once. The displacements $\{u_a\}$ for the modified structure were written as

$$\{u_a\} = \{\bar{u}_a\} + \{\delta u_a\} \tag{A7}$$

where the change in displacements $\{\delta u_a\}$ was obtained from Eqs. (A2) and (A4) and was

$$\{\delta u_a\} = -[L]^{-T}\ [M]\ \{u_b\} \tag{A8}$$

where $[M] = [L]^{-1}\ [K_{ab}]$. The displacements $\{u_b\}$ were obtained by solving Eq. (A3) together with Eqs. (A4), (A7), and (A8) and were given by

$$[K_{bb} - M^T M]\ \{u_b\} = \{F_b\} - [K_{ab}]^T\ \{\bar{u}_a\} \tag{A9}$$

Solving Eq. (A9) for $\{u_b\}$, the change in the displacements in the remainder of the structure $\{\delta u_a\}$ was obtained from Eq. (A8).

This procedure for determining the modified displacements has the advantage that the complete stiffness matrix $[K]$ does not have to be reformulated whenever the crack grows, or the crack surfaces contact or separate. However, the procedure does involve reformulation of the matrices $[K_{ab}]$ and $[K_{bb}]$ which are, generally, chosen to be much smaller than the matrix $[K_{aa}]$. A discussion on the efficiency of this procedure is comparison to a complete reformation of the stiffness matrix is given in Ref. 7.

References

[1] Elber, W., "The Significance of Fatigue Crack Closure," ASTM STP-486, May 1971, American Society for Testing Materials, Philadelphia, Pa.

[2] Elber, W., "Fatigue Crack Closure Under Cyclic Tension," *Engineering Fracture Mechanics*, Vol. 2, July 1970, pp. 37-46.

[3] Kobyashi, A. S., Chiu, S. T., and Beeuwkes, R., "A Numerical and Experimental Investigation on the Use of the J-Integral," *Engineering Fracture Mechanics*, Vol. 5, June 1973, pp. 293-306.

[4] Anderson, H., "The Steadily Growing, Elastic-Plastic Crack Tip in a Finite Element Treatment," *International Journal of Fracture*, Vol. 9, April 1973, pp. 231-233.

[5] Isakson, G., Armen, H., Jr., and Pifko, A., "Discrete-Element Methods for the Plastic Analysis of Structures," CR-803, Oct. 1967, NASA.

[6] Armen, H., Jr., Pifko, A., and Levine, H. S., "Finite Element Analysis of Structures in the Plastic Range," CR-1649, Feb. 1971, NASA.

[7] Argyris, J. H. and Roy, J. R., "General Treatment of Structural Modifications," *Journal of the Structures Division, Proceedings of the ASCE*, American Society of Chemical Engineering, Vol. 98, No. ST2, Feb. 1972.

[8] Kavlie, D. and Powell, G. H., "Efficient Reanalysis of Modified Structures," *Journal of the Structures Division, Proceedings of the ASCE American Society of Chemical Engineering*, Vol. 97, No. ST1, Jan. 1971.

[9] Armen, H., Levine, H., Pifko, A., and Levy, A., "Nonlinear Analysis of Structures," CR-2531, March 1974, NASA.

[10] Jennings, A. and Tuff, A. D., "A Direct Method for the Solution of Large Sparse Symmetric Simultaneous Equations," *Large Sparse Sets of Linear Equations*, Academic Press, New York, 1971.

[11] Vaughan, D. K., "A Comparison of Current Work-Hardening Models Used in the Analysis of Plastic Deformations," M.S. thesis, Aerospace Engineering Department, Dec. 1973, Texas A and M University, College Station, Texas.

[12] Katcher, M., "Crack Growth Retardation Under Aircraft Spectrum Loads," *Engineering Fracture Mechanics*, Vol. 5, Dec. 1973, pp. 793-818.

[13] Matthews, W. T., Baratta, F. I., and Driscoll, G. W., "Experimental Observation of a Stress Intensity History Effect Upon Fatigue Crack Growth Rate," *International Journal of Fracture*, Vol. 7, June 1971, pp. 224-228.